

# Hyperelastic piezoresistive nanocomposites for smart wearable applications

*Alejandro Triay*<sup>1</sup>, *Nikolas Savio*<sup>1</sup>, *Shanmugam Kumar*<sup>1\*</sup>

<sup>1</sup>University of Glasgow, James Watt School of Engineering, G12 8QQ, Scotland

**Abstract.** This study demonstrates the piezoresistive behaviour of hyperelastic silicone/CNT nanocomposites for large strain sensing applications. Four different 2D lattices, namely the Hexagonal, Re-entrant, I-shape and S-shape are employed to explore the effect of unit cell architecture on gauge factor. The lattices are produced at three different relative densities (30%, 40%, 50%) to determine the effect of such on piezoresistive sensitivity. Piezoresistive gauge factors of 2.66, 0.61, 4.91 and 0.20 at 125% strain were recorded respectively for each lattice geometry: Hexagonal, Re-entrant, I-shaped, and S-shaped. The results showed the effective sensitivity of the elastomeric nanocomposite auxetic lattices up to 400% tensile strain, far beyond that achieved by extant studies.

## 1 Introduction

Global advances in health and fitness have resulted in a drive for wearable monitoring devices capable of transmitting real-time information of the state of the human body. Smart wearable devices are becoming increasingly popular and have encouraged the development of smart textiles to aid in this type of monitoring. Incorporating strain sensing into wearable technology could allow for the live monitoring of breathing patterns in medical patients or movement characteristics in athletes. Conventional strain gauges tend to have a working range of between 5-20%, insufficient for the tracking of large deformations in textiles and wearable technology. They also tend to have higher mechanical stiffness which may hinder natural movement. Elastomers are known for their hyperelastic mechanical behaviour and large compliance, which would suit the objective of the application. However, neat elastomers lack the electrical piezoresistive properties needed in a strain sensor. To achieve this, the elastomer can be doped with conductive fillers which form an electrically conductive composite material. Carbon allotropes are commonly used to give electrical properties to polymers [1][2][3]. Carbon black, graphene nanoplatelets and carbon nanotubes (CNTs) are some of the used fillers in this field. This project experimented with these three carbon structures and determined the CNTs to be the most effective solution requiring the lowest weight percentage (%wt.) of filler. The CNTs form an electrical percolation network through the composite by which electrons can flow along the length of the CNTs and jump from one CNT to another through the phenomenon known as the electron tunnelling effect. CNTs are

---

\* Corresponding author: [msv.kumar@glasgow.ac.uk](mailto:msv.kumar@glasgow.ac.uk)

particularly successful at forming these networks due to their high aspect ratios of  $\sim 3000$  and conductivity of  $\sim 10^4 - 10^6$  S/cm [1].

The combined material properties of elastomers and CNTs provide the basis of this research in large-range strain sensing. To further explore potential sensor configurations, a series of 2-dimensional lattices were used to adapt the piezoresistive gauge factor sensitivity to different levels of strain. These are depicted in **Fig. 1**.

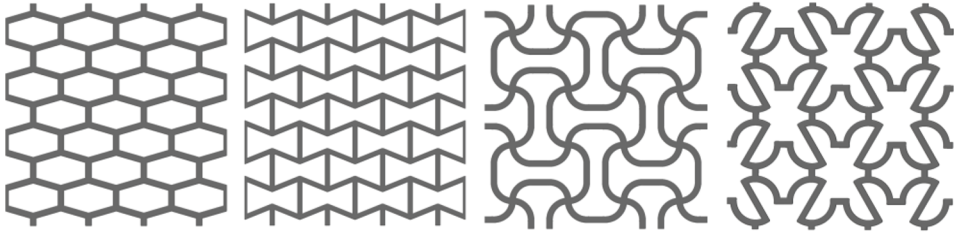


**Fig. 1.** 2-Dimensional lattices used in this project (from left to right: Hexagonal, Re-entrant, I-shaped, S-shaped).

These geometries change the sensitivity of the material at different ranges of strain. Piezoresistance in this type of composite happens due to the stretching of the percolation network of CNTs. With the use of auxetic geometries (negative poisson's ratio, as in found in the Re-entrant, I-shaped, and S-shaped structures), it is possible to delay the stretching of the percolation network to favour sensing at higher strain ranges and further increase compliance.

## 2 Materials and Methods

### 2.1 Materials

#### 2.1.1 Ecoflex hyperelastic resin

A commercial platinum cured silicone rubber resin compound was selected from *Smooth-On Inc.*: *Ecoflex<sup>TM</sup> 00-20* which proved to achieve extreme strain compliance of up to 483% under tensile testing before failure. Two monomeric parts (Part A and Part B) of the elastomer were mixed in a 50/50 ratio to produce the curing resin. To facilitate the introduction of the resin into moulds, *Smooth-On's Silicone Thinner<sup>TM</sup>* was used to reduce the viscosity of the uncured resin. The resulting mixture was 45% Part A, 45% Part B, and 10% thinner by weight. The resin was left to cure in moulds for 24 hours to ensure the process was complete before extracting the cured samples.

#### 2.1.2 Carbon nanotubes

To provide the elastomer with the required electrical properties, CNTs were mixed into the resin. The CNTs used were produced by *Applied Nanostructured Solution, LLC*. These were clusters of multi-walled-carbon-nanotubes which were grown in a chemical vapor deposition environment onto glass microfiber substrates [4].

### 2.1.3 Composite Ecoflex/CNT resin

CNTs were added into Part A of the resin before the curing process commenced to allow for their proper dispersion. CNTs tend to agglomerate and so the mixtures were ultrasonicated for 4 hours with intervals to allow for stirring. The resin thinner was also introduced during the stirring process to ease the dispersion of CNTs. The CNTs caused an increase in the bulk stiffness and strength of the final composite elastomer as shown in Table 1. The material was characterised under tensile and compressive loads and in planar tension following ISO527 to determine its shear properties for use in material modelling.

**Table 1.** Tensile properties of the neat and composite elastomer

| Material       | Elastic Modulus (MPa) | Tensile Strength (MPa) |
|----------------|-----------------------|------------------------|
| Ecoflex (neat) | 0.0481±0.0028         | 0.2249±0.009           |
| Ecoflex + CNTs | 0.1280±0.0037         | 0.3373±0.0308          |

The percolation threshold of CNTs in the elastomer was determined through examining the conductivity of the composite at varying weight percentages of CNTs in the composite. The conductivity of the composite above percolation can be fitted using the power law equation (1).

$$\sigma = \sigma_0(\rho - \rho_c)^\beta \quad (1)$$

Where  $\sigma$  is the electrical conductivity of the composite epoxy,  $\sigma_0$  is the intrinsic conductivity constant of the CNT,  $\beta$  is the critical exponent constant of the mathematical equation,  $\rho$  is the actual weight fraction of CNTs in the epoxy and  $\rho_c$  is the critical weight fraction (percolation threshold) required to form the conductive network. Linear regression data fitting was performed on the conductivity results plotted on a logarithmic scale to determine the critical exponent ( $\beta = 0.39$ ).

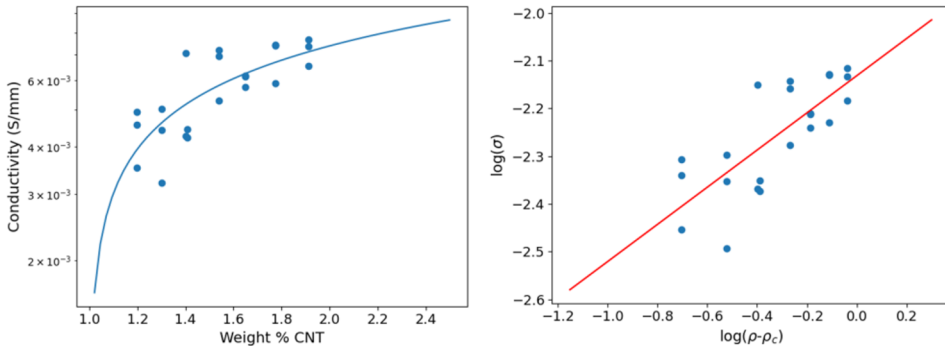


**Fig. 2.** Left: Power law fitted to the conductivity of *Ecoflex* with varying wt. % of CNTs plotted on logarithmic scale above percolation threshold. Right: Logarithmic graph adapted from power law equation to determine the critical exponent of the equation  $\beta=0.39$ .

## 2.2 Experimental methods

### 2.2.1 Mould production

Moulds for the resin were 3D printed in polylactic acid (PLA) using a *Flashforge Creator Pro 2* printer and its corresponding commercial slicer *Flashprint*. **Fig. 3** shows the workflow for the preparation of samples.

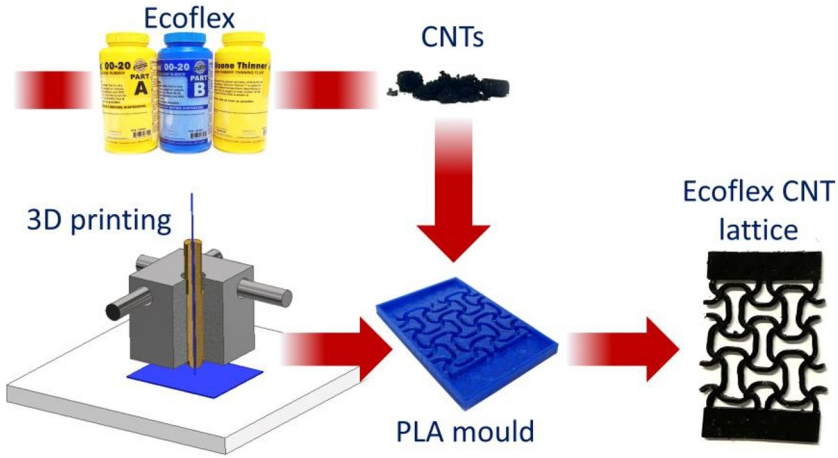


**Fig. 3.** Ecoflex/CNT sample preparation workflow

### 2.2.2 Experimental procedure

All mechanical testing (tensile, compressive, shear) was carried out using a Zwick Roell universal testing machine with a 2.5kN load cell. Experiments were carried out under quasi-static conditions at a speed of 2mm/min. Electrical resistance readings were recorded using a Fluke 8864 Precision multimeter.

## 3 Results

We can see from the results in **Table 2** that the mechanical properties of the lattices increase with the relative density as expected, with the Hex geometry performing the best overall. This is as expected as it is the only non-auxetic structure and as such its deformation is stretch dominated rather than bend dominated from the very beginning, making it less compliant to deformation and its modulus larger. Its strength is also the highest as it has the greatest number of parallel load-carrying ligaments through the structure to distribute that load and reduce localised stress.

**Table 2.** Properties of lattice structures

| Geometry | Relative density (%) | Elastic Modulus (MPa) | Tensile strength (MPa) | Gauge Factor k at 125% strain |
|----------|----------------------|-----------------------|------------------------|-------------------------------|
| Hex      | 30                   | 0.0190±0.0010         | 0.0265±0.0035          | 2.9517±0.9413                 |
| Hex      | 40                   | 0.0251±0.0019         | 0.0392±0.0048          | 2.6341±1.7192                 |
| Hex      | 50                   | 0.0313±0.0038         | 0.0484±0.0022          | 2.3857±1.6742                 |
| Re       | 30                   | 0.0094±0.0011         | 0.0168±0.0014          | 0.5038±0.1158                 |
| Re       | 40                   | 0.0146±0.0011         | 0.0247±0.0012          | 0.6247±0.2754                 |
| Re       | 50                   | 0.0322±0.0122         | 0.0372±0.0068          | 0.7062±0.2892                 |
| I        | 30                   | 0.0202±0.0046         | 0.0213±0.0047          | 3.8338±2.4162                 |
| I        | 40                   | 0.0259±0.0026         | 0.0264±0.0064          | 5.9801±5.4806                 |
| I        | 50                   | 0.0237±0.0022         | 0.0355±0.0015          | 4.8906±1.9381                 |
| S        | 30                   | 0.0091±0.0020         | 0.0162±0.0035          | 0.0903±0.0310                 |
| S        | 40                   | 0.0164±0.2323         | 0.0213±0.0036          | 0.2562±0.1483                 |
| S        | 50                   | 0.0196±0.0086         | 0.0360±0.0073          | 0.2534±0.1937                 |

Representative curves for the stress-strain behaviour of the lattices are shown in **Error! Reference source not found.** The structures with the lowest stiffness also showed the most compliance in overall strain before failure.

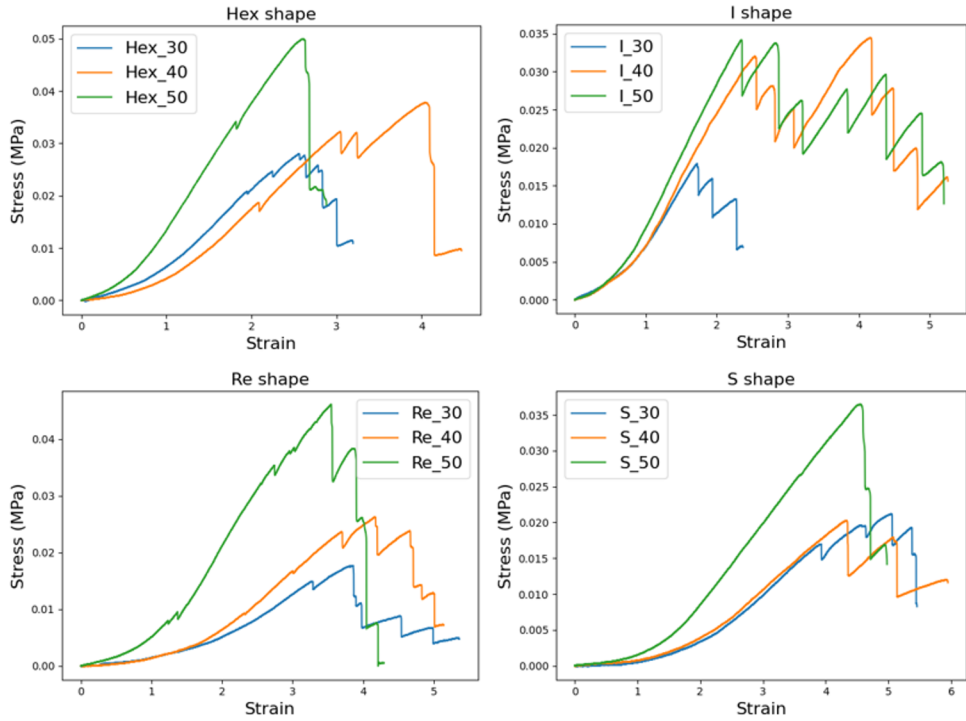


**Fig. 4.** Representative stress-strain curves for each lattice geometry at each relative density.

The piezoresistive gauge factors in **Table 2** were calculated following equation (2). Where  $\Delta R$  is the change in resistance,  $R_0$  is the initial resistance and  $\varepsilon$  is the strain.

$$k = \frac{\Delta R}{R_0 \Delta \varepsilon} \quad (2)$$

An example piezoresistive curve is provided in Figure 5 for each geometry. The more a geometry's deformation under tension is dominated by bending, the more its gauge factor is reduced due to the reduction in stretching of individual ligaments in the lattice. It is the stretching of these ligaments that produces the most significant effect on the CNT percolation network and directly influences the piezoresistive sensitivity of the material.

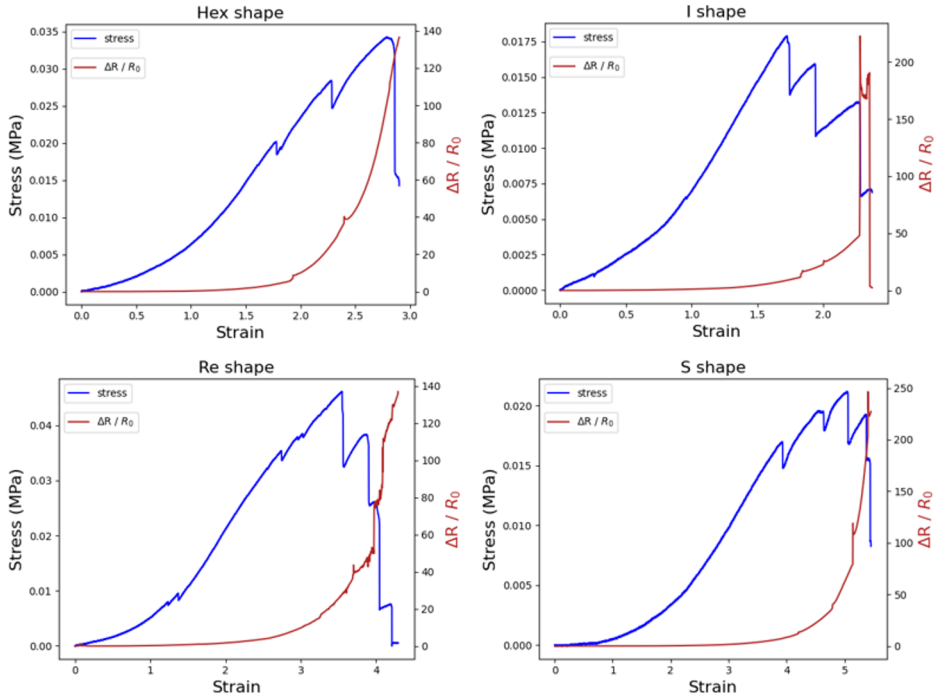


Figure 5. Example piezoresistive curve for each lattice geometry.

## 4 Conclusions

In this study, we have demonstrated the suitability of the silicone elastomeric resin doped with CNTs for use in large strain sensing applications up to 400%. The possibility of varying the unit cell architectures and relative density of the lattices allows for the tunability of gauge factor and optimisation of the mechanical properties to provide larger sensitivity at the objective strain range and stretchability over the full range of deformation required to monitor.

## References

1. P. Verma, J. Ubaid, K. M. Varadarajan, B. L. Wardle, and S. Kumar, *ACS Appl. Mater. Interfaces*, vol. **14**, no. 6, pp. 8361–8372, (2022)
2. M. F. Arif, H. Alhashmi, K. M. Varadarajan, J. H. Koo, A. J. Hart, and S. Kumar, *Compos. Part B Eng.*, vol. **184**, p. 107625, (2020)
3. A. Mora, P. Verma, and S. Kumar, *Compos. Part B Eng.*, vol. **183**, p. 107600, (2020)
4. T. K. Shah *et al.*, *Carbon nanostructures and methods of making the same*, U.S. Patent 20140093728A1, Apr. 3, 2014.